

SYNCHRONIZED MID-INFRARED PULSES AT THE FRITZ HABER INSTITUTE IR-FEL

R. Kießling, S. Gewinner, W. Schöllkopf, M. Wolf, A. Paarmann
Fritz-Haber-Institut der Max-Planck-Gesellschaft, Berlin, Germany

Abstract

The combined application of FEL radiation and femtosecond table-top lasers for two-color spectroscopy demands an accurate pulse synchronization. In order to employ the infrared FEL at the Fritz Haber Institute for non-linear and time-resolved experiments, an RF-over-fiber-based timing system has been established. Using a balanced optical cross-correlation scheme, we determined an FEL micro-pulse timing jitter of 100 - 200 fs (rms). The long-term timing drift was found to be well correlated to the energy fluctuations of the accelerated electron bunches.

By means of sum-frequency generation cross-correlation, we directly measure the FEL pulse shape at different cavity detunings. For large cavity detuning, narrowband IR radiation ($\sim 0.3\%$ FWHM) can be generated and utilized for high-resolution non-linear spectroscopy. On the other hand, sub-picosecond pulses are provided at small detuning, which are well-suited for time-resolved measurements. At intermediate detuning values, we observe the build-up and dynamics of multipulses that result in the well-known limit-cycle power oscillations.

INTRODUCTION

Vibrational excitations are a fundamental property of molecules, clusters and solids and therefore contain material-specific information. Modes of vibrations carry kinetic energy of few meV, consequently optical excitation demands infrared (IR) wavelengths. Since its first demonstration, free-electron lasers are an ideal tool for infrared spectroscopy due to the frequency-tunable narrow-bandwidth radiation output. So far, the infrared FEL at the Fritz Haber Institute (FHI) has been used to investigate (static) vibrational spectra of gas-phase ions, bio-molecules, metal-clusters and polar dielectrics. Further investigations will employ the intense FEL IR radiation also for non-linear and time-resolved two-color spectroscopy experiments. To that end, an accurate synchronization of FEL and table-top laser pulses is required for sub-ps resolved measurements. In the following, the concept, timing stability and first application of the synchronized laser system is presented.

EXPERIMENTAL SYSTEM

Free-Electron Laser

Since the start of user operation in 2013, the mid-IR free-electron laser oscillator at the FHI provides intense, pulsed radiation in the wavelength region from 3 to 50 μm [1]. The electron bunches emitted from a thermionic cathode are accelerated by two subsequent normal-conducting linacs to

kinetic energies between 15 and 50 MeV, depending on the desired IR spectral range. The master oscillator (MO), an 2.99 GHz RF source, drives the electron gun at the third sub-harmonic, producing few-ps short micro-bunches of 1 GHz repetition rate within $\sim 10\ \mu\text{s}$ long macro-bunches at a 10 Hz rate. The following electron wiggling in a planar hybrid-magnet undulator with parameter $K = 0.5 - 1.6$ generates linearly polarized, ps-long IR pulses with a gap-scan tunable wavelength. Besides a 1 GHz micro-pulse rate, reduced repetition modes of 27.8 MHz and 55.5 MHz are available that are required for time-resolved studies. Adjustment of the optical cavity length is an additional degree of freedom to set the spectrum bandwidth as low as 0.3 %.

Synchronization Setup

As table-top laser we employ a high-power Terbium-doped fiber oscillator (FO) providing ~ 100 fs, near-infrared ($\lambda = 1055$ nm) pulses with up to 50 nJ pulse energy. The repetition rate of 55.5 MHz is matched to a reduced electron micro-bunch rate, corresponding to two FEL pulses circulating in the 5.4 m long FEL cavity simultaneously. For high-precision synchronization, the MO signal of 2.99 GHz is distributed from the FEL vault to the user lab via a stabilized RF-over-fiber link approximately 100 m long. This reference clock transfer system is a low-jitter (rms < 7 fs [10 Hz-10 MHz]) and low-drift (< 40 fs/day) RF transmission turn-key solution utilizing optical fiber connections [2].

The FO is locked to the MO using the 54th harmonic of the table-top laser output. Adjustment of the FO repetition-rate is done by temperature control of the fiber cage for coarse tuning and a piezo motor for fine setting of the fiber cavity length. In order to manage multiple synchronized situations due to phase-locking of the table-top laser to a higher frequency reference clock, a phase-shifter of the 2.99 GHz signal is added using the photodiode signal of the FO and a separately fiber-link transferred 55.5 MHz RF signal from the FEL machine (superperiod-lock). The shifter is used to adjust the temporal overlap of the optical pulses in the experimental setup. The fiber cables of the synchronization system going along the beamline from the FEL vault to the user lab are subject to ambient temperature and humidity fluctuations, which are compensated by the system.

Balanced Optical Cross-Correlation

Characterization of the synchronization stability of the FEL-table-top laser system is performed by two-color balanced optical cross-correlation (BOC) [3]. Utilizing a non-linear crystal (GaSe) for sum-frequency generation (SFG), the FEL and fiber oscillator pulses are overlapped twice within the same crystal, but with slightly different temporal

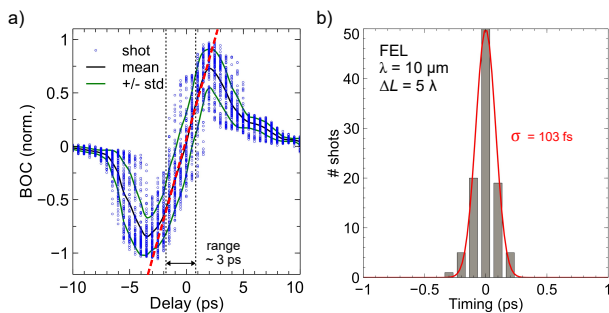


Figure 1: Jitter determination by balanced optical cross-correlation. (a) Measured BOC curve by scanning the FEL-table-top laser pulse delay τ with 100 FEL macro-pulses per delay point. The linear dynamic range of the tool is about 3 ps. Analysis of the delay value at zero BOC crossing informs about the timing, which is shown in the histogram plot in (b). By fitting a Gaussian distribution, a jitter value of $\sigma \sim 100$ fs (rms) is extracted.

overlap Δt . After separation of both SFG signals from the fundamental pulses, the balanced cross-correlation value is obtained by normalizing and subtraction of the SFG1 and SFG2 intensity. Scanning the relative delay τ between FEL and table-top laser pulse gives the BOC curve. In contrast to a single cross-correlation, the absolute delay between the pulses is determined without sign ambiguity. For a properly chosen fixed time delay Δt , the BOC signal is linear within a certain range around $\tau = 0$. By statistical analysis, the FEL shot-to-shot micro-pulse timing jitter can be extracted from the shift of the zero-crossing position. The slope of a linear fit near the zero-crossing provides the calibration coefficient of the BOC curve. Setting the time τ to a constant value within the center of the linear range and converting the BOC value measured over a long period of time into a temporal information offers the timing drift of the FEL micro-pulses with respect to the FO pulses. Results shown below were obtained at a FEL wavelength of $10 \mu\text{m}$ with $\sim 1 \mu\text{J}$ micro-pulse energy at a repetition rate of 27 MHz (or 1 GHz, respectively) and ~ 5 nJ FO pulse energy. Since phase-matched SFG is used, standard photodiodes are sufficient for signal detection.

TIMING CHARACTERISTICS

A typical shot (i.e. macro-pulse)-resolved BOC curve is shown in Fig. 1a. Analyzing 100 subsequent shots, the root mean square value of the timing shift is about $\sigma = 200 - 300$ fs in the case of 1 GHz FEL micro-pulse rate and $\sigma \sim 100$ fs in 27 MHz low-repetition mode (Fig. 1b). No (significant) dependence of the optical pulse jitter on FEL wavelength (different undulator gap size for given electron energy) or FEL cavity length (mirror translation) was found. Considering that the synchronization relies on electronic phase-locking, a high timing stability is achieved that is suitable for sub-ps resolved FEL-table-top experiments.

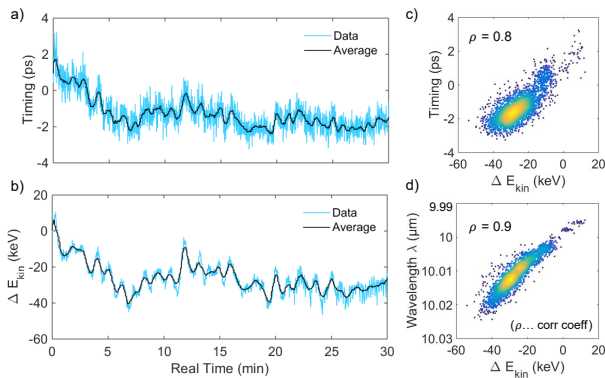


Figure 2: Drift of FEL pulse timing and energy. (a) Micro-pulse timing fluctuations measured by BOC and moving average with half minute window and (b) corresponding changes in kinetic energy of electron bunches as determined by beam-position monitoring. Nominal electron energy is 36.5 MeV. Also shown are correlation plots of kinetic energy vs. timing (c), and vs. FEL radiation wavelength (d), respectively.

The long-term temporal shift is determined to be 3 ps per 15 min peak-to-peak (Fig. 2a). Simultaneously, the kinetic energy of the accelerated electron bunches was monitored (Fig. 2b). As depicted in Fig. 2c, a clear linear correlation (coefficient $\rho = 0.8$) consists between changes of the electron energy after the two linacs (up to 0.1 %) and the timing drift. Since the magnetic undulator field is fixed during this measurement, the kinetic energy fluctuations are directly reproduced in the shift of the FEL center wavelength (Fig. 2d). Consequently, the drifting temporal overlap is mainly caused by amplitude and/or phase fluctuations in the accelerating fields of the linacs; thermal drifts in the system are of minor impact.

FEL PULSE BEHAVIOR

An application of the low-jitter synchronized laser is to study the evolution of the FEL micro-pulse shape within the macro-pulse. The measurement is done by recording the

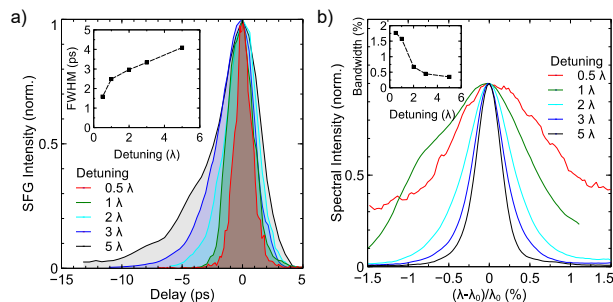


Figure 3: Cavity detuning dependence of FEL micro-pulse. (a) Temporal shape measured by SFG cross-correlation and extracted FWHM duration, (b) Spectral structure and bandwidth.

Content from this work may be used under the terms of the CC BY 3.0 licence (© 2018). Any distribution of this work must maintain attribution to the author(s), title of the work, publisher, and DOI.

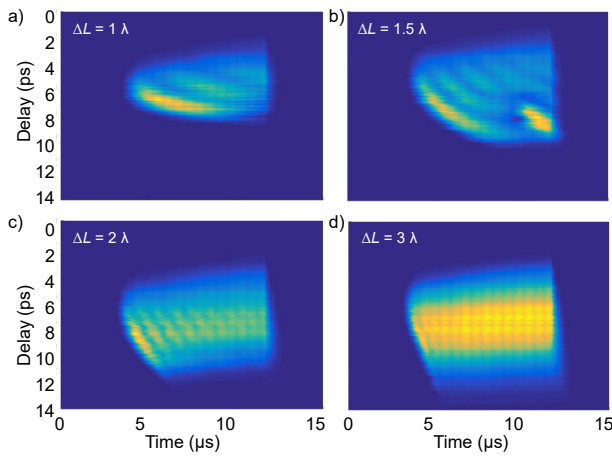


Figure 4: Evolution of the micro-pulse shape within a macro-pulse of the FEL oscillator for different cavity detunings ΔL . Data are measured by SFG cross-correlation. The optical macro-pulse is about 10 μs long, ending at around 12 μs .

(single) sum-frequency cross-correlation intensity during a complete macro-pulse while scanning the delay between FO pulse and FEL micro-pulse. Since the temporal duration of the FO pulse is much shorter than that of the FEL micro-pulse, the SFG signal resembles the actual intensity envelope of the FEL pulse. The dependence of the pulse shape on the cavity detuning is depicted in Fig. 3a. While the electron macro- and micro-bunch durations are unchanged, the length of the optical micro-pulses increases for larger detuning values. The corresponding narrowing of the spectral bandwidth can be observed in Fig. 3b. Additionally, there is a transition from a Gaussian to an asymmetric micro-pulse shape with an exponential leading edge. This behavior is caused by a change of the temporal overlap between the short optical pulses and electron bunches [4]. Shorter cavity lengths shift the free electron gain medium to the edge of the IR pulse that is amplified.

Further details of the pulse evolution are revealed by analyzing the completely delay- and time-resolved SFG cross-correlation data, shown in Fig. 4 and 5a, where the FEL cavity detuning is a highly sensitive parameter. At the beginning of the macro-pulse, optical micro-pulses begin to develop until a steady-state duration and intensity saturation is reached after a number of undulator passes. The temporal end of the macro-pulse lasing is mainly determined by the electron macro-bunch switch-off, but also dependent on the cavity quality factor. For small detunings, pronounced power oscillations within a macro-pulse appear. Period and strength of the intensity modulation (up to 50%) diminish with increasing cavity detuning.

The power oscillations result from the formation of equally-spaced sub-pulses within a micro-pulse as can be seen in cross-correlation (Fig. 5b) as well as auto-correlation delay scans (Fig. 6). These so-called 'limit-cycle' oscillations (Fig. 5c) were previously observed also at another IR FEL oscillator as a consequence of the short optical and elec-

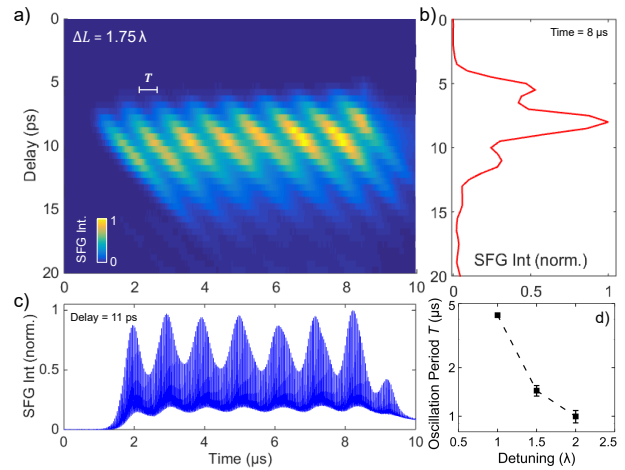


Figure 5: FEL pulse shape in the case of limit-cycle oscillations obtained by cross-correlation measurement. The cross-sections from the 2D plot in (a) along a constant time of 8 μs within the macro-pulse (b) and a constant delay of 11 ps (c) clearly show the sub-pulse structure of the micro-pulses and power oscillations within the macro-pulse, respectively. The dependence of the oscillation period on the cavity detuning is depicted in (d).

tron pulses [5]. Due to a velocity difference the optical pulse at saturation loses temporal overlap with the electron bunch. Only at the trailing edge the optical micro-pulse undergoes amplification, resulting in the growth of a sub-pulse. The repeated modulation of the optical group velocity results in the periodic sub-pulse formation as long as there is net gain. Larger detuning values result in lower saturated power so that the modulation depth decreases until a stable output regime with a uniform single long micro-pulse is settled (Fig. 6d).

In contrast to previous experimental investigations of limit-cycle oscillations based on power or auto-correlation measurements (e.g., [5, 6]), the cross-correlation study presented here allows one to follow the evolution of the sub-pulses during subsequent cavity round-trips (i.e., along the macro-pulse timescale). It can be clearly seen how the sub-pulse structure initiates on the trailing edge of the optical micro-pulse and is shifted through the pulse envelope over many passes. The agreement with simulations based on Maxwell-Lorentz theory [6] is apparent.

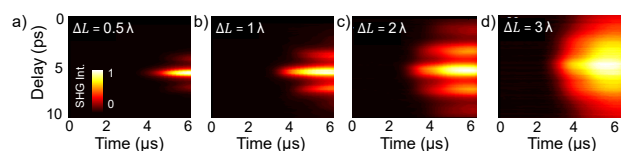


Figure 6: Sub-pulse structure measured by second-harmonic generation (SHG) auto-correlation of the FEL micro-pulses for different detunings ΔL . For shorter cavity lengths, more sub-pulses are formed until their overlap results in a single-peaked long micro-pulse.

CONCLUSION

We implemented a low-jitter ($\sigma \sim 100$ fs) synchronization of a NIR femtosecond table-top laser oscillator to the MIR FEL operating in the wavelength region of 3 to 50 μm at 27 MHz, 55 MHz or 1 GHz repetition rate. This enabled us to study the optical micro- and macro-pulse intensity shape and duration of the FEL by cross-correlation measurements in great detail. In particular, our observations confirm the strong dependence on the cavity detuning. The high-resolution scans clearly resolve the occurring limit-cycle oscillations and sub-pulse formation. Furthermore, the study provides useful information for our ongoing efforts to utilize the short-pulsed FEL radiation for time-resolved spectroscopy.

REFERENCES

- [1] W. Schöllkopf *et al.*, in *Proc. SPIE* 9512, 95121L (2015).
- [2] S. Zorzut *et al.*, in *Proc. FEL2015*, paper MOP043, p.126 (2015).
- [3] S. Schulz *et al.*, *Nat. Commun.* 6, 5938 (2015).
- [4] G. M. H. Knippels *et al.*, *Phys. Rev. Lett.* 83, 1578 (1999).
- [5] D. A. Jaroszynski *et al.*, *Phys. Rev. Lett.* 70, 3412 (1993).
- [6] D. A. Jaroszynski *et al.*, *Nucl. Instr. Meth. Phys. Res. A* 331, 52 (1993).